# POTASSIUM ION CURRENTS IN THE CRAYFISH GIANT AXON

## DYNAMIC CHARACTERISTICS

STEVEN H. YOUNG AND J. W. MOORE, *Department of Physiology, Duke University Medical Center, Durham, North Carolina 27710.*

ABSTRACT The kinetics of the voltage-sensitive potassium channel in crayfish axon have been examined. The conductance increase after a step depolarization from rest can be described by a first-order kinetic process raised to the third power. When conditioning voltage levels preceded the test pulse, the steady-state conductance was found to be independent of initial conditions. Depolarizing conditioning voltages in general allowed superposition of test voltage potassium currents by a shift along the time axis. Hyperpolarizing conditioning voltages produced a delay in onset of conductance during the test pulse and changed the kinetics so that superposition was not possible. The delay increased during the hyperpolarization with a first-order lag having a time constant in the range of 1.5–3 ms. Return to the resting level caused recovery from the delayed state to follow a single exponential decay with a time constant of 1.9–2.2 ms. The steady state delay vs. voltage curves were not saturated at potentials as negative as −180 mV.

### INTRODUCTION

Hodgkin and Huxley (1952, hereafter referred to as HH) described the kinetics of the potassium current in squid axon membranes in a voltage clamp by a single variable $n$ raised to the fourth power, where $n$ obeys a first-order linear differential equation. Cole and Moore (1960*a*) examined the adequacy of such a single voltage-sensitive variable description by testing for superposition, i.e., will the currents resulting from a step to a given test potential from any initial condition superpose with only a shift in time? They found that superposition held under all initial conditions, in spite of the fact that large conditioning hyperpolarizations produce a marked delay in the onset of current. These results have been confirmed and extended for a greater range of test potentials by Moore and Young (1981).

Other axonal preparations have been tested for superposition. In the giant axon of *Myxicola*, superposition holds under all initial conditions (Schauf, et al., 1976). In the node of the frog, with hyperpolarized conditioning, superposition of test potential currents was not possible (Palti et al., 1976; Begenisich, 1979). The frog node preparation then exhibits a property fundamentally different from that of squid: the potassium current kinetics cannot be described by a single variable. In earlier work on crayfish axons, Shrager (1974) presented a single figure showing a delay in $g_k$ onset with hyperpolarized conditioning levels. The author

---

Dr. Young's present address is Department of Physiology and Biophysics, University of California at Irvine, Irvine, California 92717.

does not comment on superposition but it does not appear to hold in the small published figure.

We have carried out experiments on the crayfish giant axon (*a*) to examine and describe its kinetics systematically, and (*b*) to see if potassium current superposition holds in this preparation. We found that the HH variable $n$ raised to the third power is sufficient to describe its kinetics from rest. We also found that depolarizing conditioning pulses allow superposition of the test pulse currents but, as in frog node, hyperpolarizing conditioning does away with superposability. We describe two models that reproduce the general features of this behavior.

## METHODS

An axial wire voltage clamp was used in these experiments and is described in detail in a PhD dissertation (Young, 1980). The nerve cord of the crayfish *Procambarus clarkii* contains two large axons, the medial giant axons, which are unbranched through most of the length of the cord, and are of sufficient diameter to permit insertion of an axial electrode. The cord was removed from the animal and pinned out in a dissecting dish. Connective tissue, cord sheath, and ganglia were removed from the thoracic region, where the axon diameter is ~150 μm.

The internal electrode consisted of a platinized 25-μm-diameter 90% Pt–10% Ir wire cemented to a 50-μm o.d. glass cannula that contained an 18-μm floating Pt wire to reduce the impedance of the cannula (Hodgkin and Katz, 1949). The surface impedance of the axial wire was reduced to 2–3 $\Omega cm^2$ (referred to membrane area, Cole and Moore, 1960*b*) by platinizing. The cannula was filled with an electrode solution composed of 172 mM KCl and 37 mM $K_3$ citrate titrated to pH 7.5 with citric acid (Shrager, 1974). A liquid junction potential correction of 5 mV was made. Compensation for 70–90% of the series resistance was used.

The external solution was Van Harreveld's (1936) saline buffered with 5 mM Hepes and titrated to pH 7.5 with NaOH. To block sodium current, tetrodotoxin (TTX) at 100 nM was added to the external solution (Moore and Narahashi, 1967). Temperatures ranged from 6 to 10°C. Leakage current was subtracted by an electronic bridge circuit.

## RESULTS

### *Normal Potassium Conductance Dynamics*

Records of membrane potassium current in response to depolarizing potential steps were stored in digital form on magnetic tape. A least-squares curve-fitting program on a PDP-15 computer (Digital Equipment Corp., Maynard, Mass.) obtained the parameters for the best fit to the HH description of the potassium conductance $\bar{g}_k n^x$. Various values for $x$ were tried to fit the data for test pulses from rest. Although no given value of $x$ gave an exact fit to records from all voltage levels, the best overall fit was obtained with $x = 3$. Shrager (1974) used $x = 5$ for his data because of "better agreement with data."

### *Tests of Superposition: General Findings*

Experiments were performed under a wide range of test voltages (0 to +35 mV) and conditioning levels (−185 to +40 mV) applied for 0.1–10 ms.

The steady-state potassium current was found to be independent of initial conditions. In general, depolarizing prepulses produced potassium currents that would superpose with a shift in time, but hyperpolarizing prepulses would not produce conditions of superposition. This statement is true for our normal range of holding potentials, −70 to −85 mV, but the

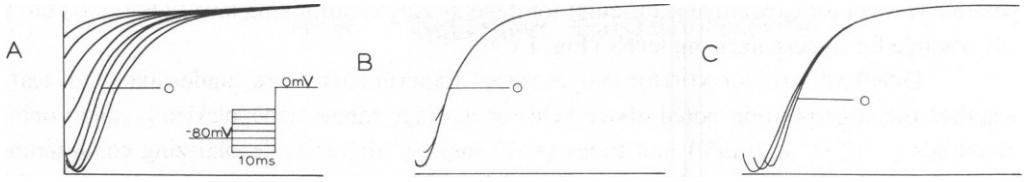


FIGURE 1 Tests for superposition of potassium currents at depolarization to 0 mV from a holding potential of −80 mV in crayfish axon JULO at 10°C. (*A*) Family of currents following 10 ms conditioning pulses to −120, −100, −80, −60, −40, and −30 mV. The curve labeled 0 indicates no deviation from holding potential. (*B*) Currents following depolarized conditioning can be superposed by shifting in time. (*C*) Currents following hyperpolarized conditioning cannot be superposed with a time shift. The maximum current is 1.15 mA/cm², and the test pulse duration is 5 ms.

property of superposition actually depends on the absolute value of the conditioning level. The polarity of a voltage pulse to achieve that level depends on the actual holding potential. Occasionally, small depolarizations from large negative holding potentials are still within the voltage range that produces non-superposition.

Fig. 1 illustrates some of these properties. Fig. 1 *A* shows tracings of the currents obtained by pulses to the test level of 0 mV. The holding potential was −80 mV. The conditioning pulses (not shown) were 10 ms long and of potentials ranging from −120 to −30 mV. All test voltage currents approach the same steady-state level to within the oscilloscope beam width, and are blended into a single line. The curve labeled "0" is obtained from a test step without a conditioning pulse. In Figs. 1 *B* and *C*, the currents are shifted in time. Superposition is

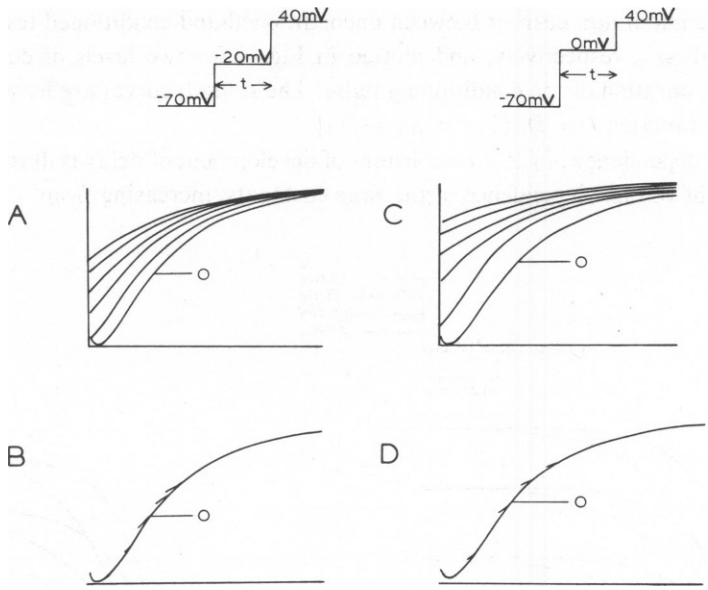


FIGURE 2 Superposition of potassium currents for a test voltage step to +40 mV after different conditioning times. (*A*) Depolarizing conditioning voltage of −20 mV, duration 0 (curve 0), 1, 2, 3, 4, and 5 ms. (*B*) The currents from *A* are shifted in time to show that superposition can be achieved. (*C*) and (*D*) Same protocol as *A* and *B*, but with a conditioning voltage of 0 mv. The maximum current is 0.5 mA/cm², and the test pulse duration is 5 ms. Axon JAN30 at 8°C.

possible (except for capacitive transients) for depolarizing conditioning levels (Fig. 1 *B*) but is not possible for hyperpolarizing levels (Fig. 1 *C*).

DEPOLARIZING CONDITIONING PULSES Experiments were undertaken to learn whether the superposition noted above held for a wider range of depolarizing conditioning potentials (−70 to +30 mV) and times (1–10 ms). In all cases, depolarizing conditioning pulses from a holding potential more positive than −75 mV produced superposable (i.e., with time shift) currents at the test potential. Two examples are shown in Fig. 2.

HYPERPOLARIZING CONDITIONING PULSES Since the lack of superposability after hyperpolarizing conditioning levels does not fit expectations of a system that follows a single-state variable, an alternative to the HH treatment must be considered. Additional experiments to study the behavior of the crayfish axon under hyperpolarized initial states were carried out in order to provide the data base to which any alternative model of potassium conductance must conform.

The characteristic distortions of the potassium current dynamics upon conditioning hyperpolarization are illustrated in Fig. 3. Fig. 3 *A* shows pairs of $I_K$ for the same test levels (−45, −25, −5, and 15 mV) with and without conditioning hyperpolarization to −145 mV for 10 ms. At each test voltage, the pairs of currents approach the same steady-state value. Hyperpolarization before the test step delays the onset of potassium conductance by a time that depends on the test voltage (smaller test potentials show larger delays). The change in onset kinetics of the delayed currents prevents superposition. Greater conditioning hyperpolarization (−185 mV) increases the delay in onset of the currents as shown in Fig. 3 *B*.

*The time-course of development of delay* To obtain some measure of the development of delay, the values of two parameters were followed. The time delays to reach 25 and 50% of the maximum current between unconditioned and conditioned test currents were called $\Delta t_{25}$ and $\Delta t_{50}$, respectively, and plotted in Fig. 4 for two levels of conditioning as a function of the duration of the conditioning pulse. The smooth curves are least-squares fits of the data to the function $D = D_\infty [1 - \exp(-t/\tau)]$.

The voltage dependence of the time constant of development of delay is illustrated in Fig. 5. There is a slight voltage dependence of the time constants, increasing from ~1.5 ms at −175

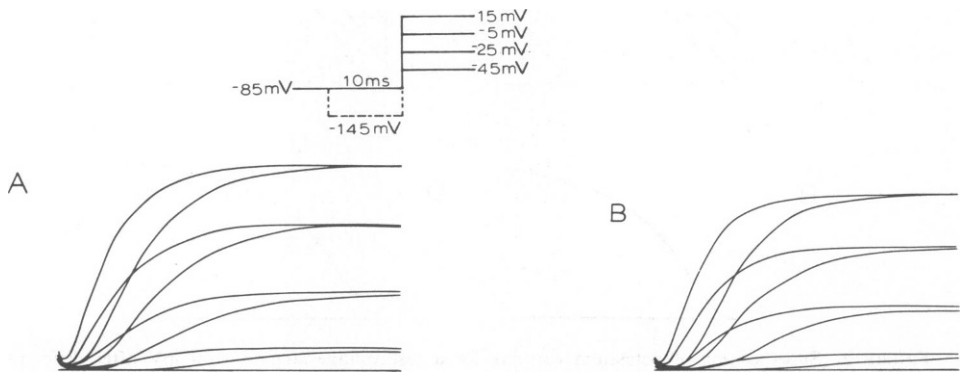


FIGURE 3 Changes in $I_k$ with 10-ms hyperpolarized conditioning voltages of (*A*) −145 mV and (*B*) −185 mV preceding test voltages of −45, −25, −5, and +15 mV. Vertical scale, 0.2 mA/cm² horizontal scale 1 ms. Axon JUN30, 9°C.

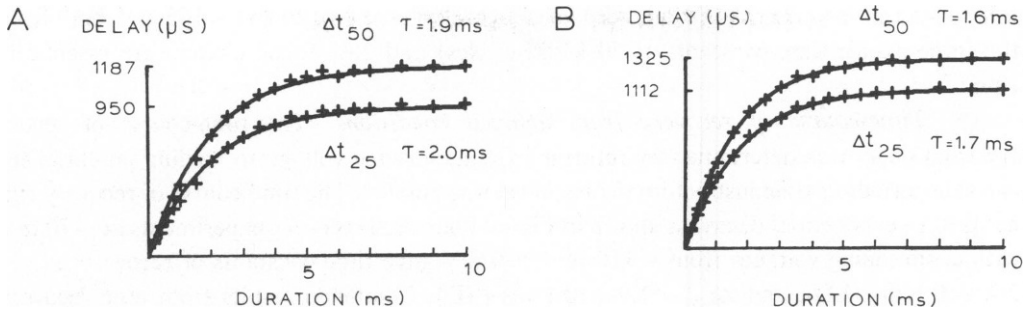


FIGURE 4 Development of delay in $I_k$ at a test voltage of +35 mV expressed as $\Delta t_{25}$ and $\Delta t_{50}$ as a function of conditioning pulse duration from a holding potential of −75 mV in axon MAR19 at 8°C. Test voltage, +35 mV. (*A*) Conditioning voltage, −155 mV. (*B*) Conditioning voltage, −175 mV.

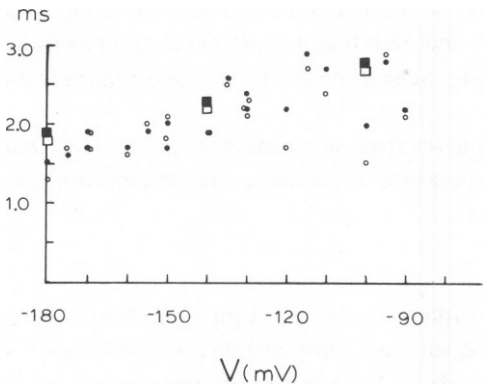


FIGURE 5 Voltage dependence of the time constant of onset of delay in $I_k$. Data from three crayfish axons at 8°, 8° and 7°C, where $\Delta t_{25}$ time constants are shown as open circles, and $\Delta t_{50}$ time constants are shown as filled circles. The filled and open squares are values computed (at 10°C) from a model of delay described in the text.

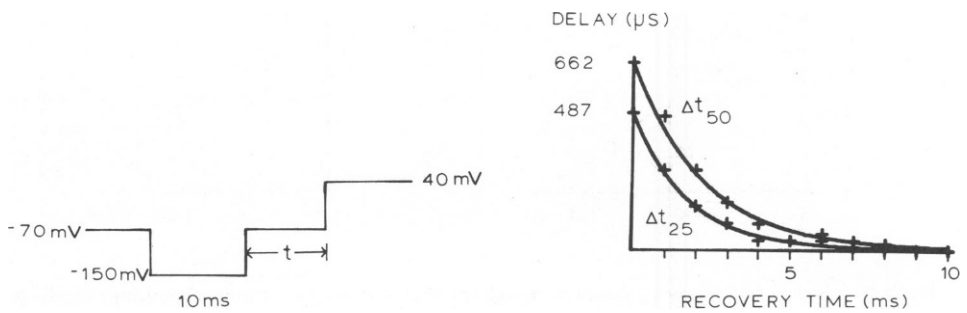


FIGURE 6 Recovery from delay. $\Delta t_{25}$ and $\Delta t_{50}$ as a function of recovery time at a holding potential of −70 mV. Axon JAN30 at 8°C.

mV to ~2.7 ms at −95 mV. Except for two values of voltage (−120 and −105 mV, both from the same axon), time constants at 50 (solid circles) and 25% (open circles) are essentially equal.

*Time-course of recovery from delayed conditions* The time-course of recovery from delay was determined by returning the membrane voltage to holding potential for variable periods of time just before the test level was applied. The time-course of recovery can be fit to an exponential decay, as shown in Fig. 6. Four such recovery experiments at −70 mV with conditioning voltages from −110 to −150 mV gave time constants of recovery $\Delta t_{50}$ = 2.2 ± 0.1 ms (SD), and $\Delta t_{25}$ = 1.9 ± 0.1 ms (SD). Combined results from nine recovery experiments show that the recovery time constant is not dependent upon the conditioning voltage. Time constants for $\Delta t_{25}$ are slightly (13%) smaller than those for $\Delta t_{50}$ at the same time voltage.

*Steady-state delay as a function of voltage* The steady state delay for any conditioning voltage was achieved by 10 ms. Fig. 7 *A* shows that steady-state $\Delta t_{25}$ and $\Delta t_{50}$ delays at test level of +30 mV are linear functions of voltage, showing no tendency towards saturation even at the most hyperpolarized level. However, the steady-state delay vs. voltage curve is not always linear and may tend toward saturation, as shown in Fig. 7 *B* for another axon for several test levels. Schrager (1974) has also reported such saturation in crayfish axons.

Examination of delay curves from other axons over a limited temperature range (6–10°C) does not indicate a temperature dependence. It remains unclear why some axons show linearity and others do not.

## DISCUSSION

The axons of all preparations so far examined—*Loligo, Myxicola, Procambarus,* and *Xenopus* and *Rana*—produce potassium currents whose kinetics under depolarizing pulses can be fit by the HH formalism. With hyperpolarizing prepulses, the crayfish and frog node membranes differ from those of squid and *Myxicola* in that they produce currents that will not superpose upon currents from control pulses with temporal translation (see also Fig. 9 of Shrager [1974]). Furthermore, the squid and *Myxicola* preparations themselves differ in the way in which the induced delay is expressed. In the squid, the exponent of a single-state

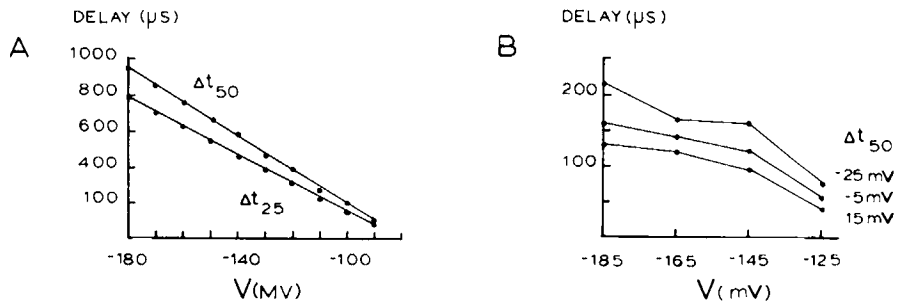


FIGURE 7 Steady state delay vs. conditioning voltage level. (*A*) A linear steady-state delay vs. voltage relation from axon MAR19 at 7°C for a test step to +30 mV from a holding potential of −80 mV. (*B*) A nonlinear relation of steady state delay vs. conditioning voltage from axon JUN30 at 9°C. Three test voltage levels, −25, −5, and 15 mV, were used from a holding potential of −85 mV.

variable according to Hodgkin and Huxley must be changed from 6 to 25 (Cole and Moore, 1960 *b*). In *Myxicola,* the exponent changes from 2 to 3 (Goldman and Schauf, 1973). The failure of superposition in the crayfish axon and frog node indicate that the single-state variable description is inadequate for these membranes.

The delayed currents from crayfish appear much like those produced in the frog node (Palti et al., 1976; Begenisich, 1979). The manner in which the delayed currents differ from control potassium currents is strikingly similar. Unlike Palti et al., Begenisich finds steady-state levels of potassium current that are independent of condtioning history. This was true for all crayfish axons examined in the present experiments. We have found that, in general, depolarizing conditioning pulses will produce superposition in the crayfish axon. Begenisich shows one record (his Fig. 2 *d* [1979]) in which a depolarizing conditioning pulse produced superposition.

The time-course of development of the delay $\Delta t_{50}$ in the frog node can be fit to a first-order lag (Begenisich, 1979). Time constants range from ~2 ms at −180 mV to ~3.5 ms at −80 mV (Begenisich, 1979). Crayfish $\Delta t_{25}$ and $\Delta t_{50}$ curves can be fit to a first-order lag, with time constants of 1.5 ms at −180 mV to 2.7 ms at −95 mV. Both preparations show a slight increase in time constants from ~2 ms for large hyperpolarizing prepulses to ~3 ms at resting potential. The experiments were performed at different temperatures (frog, 15°C; crayfish, 6–10°C).

There exists a significant difference in time constants of recovery between crayfish and frog. The crayfish recovery time constant at −80 mV is ~1.8–2.7 ms. In the frog node, recovery to rest (taken as −80 mV) takes place with a time constant in the range of 5–11 ms (Begenisich, 1979).

### *Models*

It is clear that a model of potassium conductance with a single voltage-sensitive variable will not account for the data. In constructing new models, it seems most reasonable to be conservative and start by examining models with a limited number of states.

#### *Linear Reaction Sequences*

One approach for construction of a kinetic model is to write a reaction sequence equivalent to the HH model, and then add new states or change rates in the entire sequence.

Begenisich (1979) suggests that the cooperativity models of Hill and Chen (1971*a, b*), rejected for squid because of failure of superposition, might be applied to the frog node. Simulations showed that these cooperativity models will not fit crayfish data because they cannot be made to produce both a superposition with depolarized conditioning levels while maintaining a delay in onset of conductance from hyperpolarized levels.

We noted above that the potassium conductance of crayfish membrane response to a step of depolarization from the resting level follows the cube of a first-order process. This HH expression of $n^3$ can also be written as a linear sequence

$$\mathrm{R} \rightleftharpoons 1 \rightleftharpoons 2 \rightleftharpoons \mathrm{G} \qquad \text{(Reaction 1)}$$

where R is the preferred state at rest, and G (conducting) is that preferred under depolarization. Addition of a state H, preferred during membrane hyperpolarizing, provides a

delay:

$$H \underset{\beta z}{\overset{\alpha z}{\rightleftharpoons}} R \underset{\beta_n}{\overset{3\alpha_n}{\rightleftharpoons}} 1 \underset{2\beta_n}{\overset{2\alpha_n}{\rightleftharpoons}} 2 \underset{3\beta_n}{\overset{\alpha_n}{\rightleftharpoons}} G. \qquad \text{(Reaction 2)}$$

The voltage sensitivity of the rate constants $\alpha_n$ and $\beta_n$ (in milliseconds$^{-1}$), was found by a simplex method of curve fitting (in terms of the absolute membrane potential $V$ in millivolts) to be well described as follows:

$$\alpha_n = \frac{0.016(-V69.5)}{\exp[(-V-69.5)/7]-1} \qquad \text{(Eq. 1)}$$

$$\beta_n = 0.03 \exp(-V/30). \qquad \text{(Eq. 2)}$$

The rate constants involved in the transitions between the new state H and R were determined (at 10°C) to be

$$\alpha z = 0.613 \exp(V/99.2) \qquad \text{(Eq. 3)}$$

$$\beta z = \frac{0.005(V+80)}{\exp[(V+80)/10]-1}. \qquad \text{(Eq. 4)}$$

At a holding potential of −80 mV, the fractional occupancy of state H is 0.11 of the total population of states, but this is lowered to 0.037 at −70 mV. During a strong prepulse (to −180 mV), occupancy of the H state can rise to >0.9.

This model provides an excellent reproduction of the features of kinetic changes resulting from hyperpolarizing conditioning. The computer simulations of this model shown in Fig. 8 are very similar to the experimental results in Fig. 3. The model also retains superposition for depolarizing conditioning levels, as seen in Fig. 9. These simulations are quite similar to the experimental data in Fig. 1. The development of delay can be fit to a first-order lag as shown in Fig. 10 *A*. The time constants at −180, −140, and −100 mV are plotted in Fig. 5. Recovery from delay can be fit with an exponential decay, as illustrated in Fig. 10 *B*. The time constant of the $\Delta t_{25}$ decay is 1.5 ms, and the time constant of $\Delta t_{50}$ is 2.1 ms. These numbers compare well with values from the axon at −70 mV of 1.9 ms and 2.2 ms.

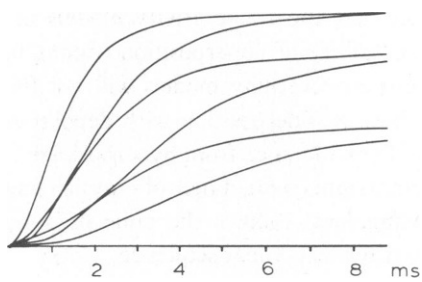


FIGURE 8 Simulation of delay and shape change following a 10-ms hyperpolarizing conditioning pulse to −180 mV. Traces of pairs of test conductances are shown, one with and one without the conditioning pulse. Test potentials are −40, −20, and 20 mV, and the maximum conductance is normalized to unity.

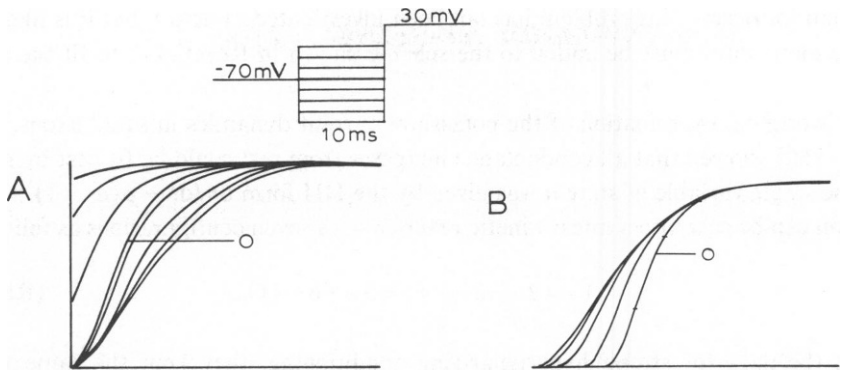


FIGURE 9 Simulation of superposition for depolarized conditioning and failure of superposition for hyperpolarized conditioning. (*A*) Simulated conductances from test steps to 30 mV from a holding potential of −70 mV with intervening 10-ms conditioning potentials of −10, −30, −50, −70, −90, −110, −130, and −150 mV. (*B*) Traces from *A* are shifted in time to test for superposition, and show that +30-mV conductances following conditioning potentials of −10 to −70 mV superpose, whereas those following −90 to −150 mV fail. The maximum conductance is normalized to unity, and the time scale is 1 ms.

The model predicts a deviation from linearity of steady state delay starting at about −140 mV, but saturation is not reached by −180 mV, as can be seen in Fig. 10 *C*.

This simple extension of the linear representation of a single-state variable model accounts for many of the observed properties of potassium channels in crayfish axon membranes. Although the model predicts saturation of delay at large hyperpolarizations, it is not possible to verify this experimentally because hyperpolarizations much beyond our maximum (−185 mV) cause membrane breakdown. However, some axons do show a nonlinearity, hinting at a saturation effect.

The usefulness of this model in describing crayfish potassium channels is evident, but it is not certain whether it will describe all of the properties of potassium channels in frog node. In the crayfish, the time constants (for small hyperpolarizations) for onset and recovery from delay are about equal. In the frog node, the time for recovery from delay is two- to threefold

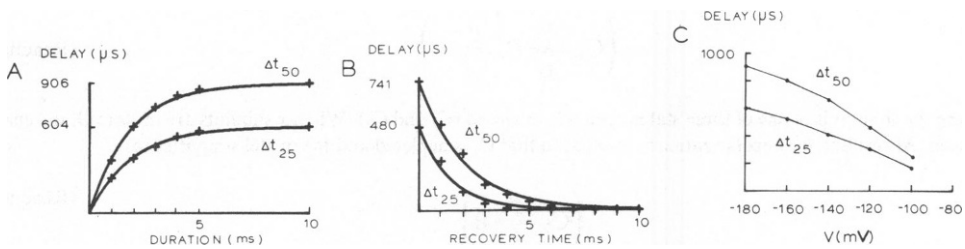


FIGURE 10 Simulation of development and recovery from hyperpolarization delay. (*A*) Development of delay at a test level of +20 mV following a conditioning voltage of −180 mV. The curves are least-squares fits to the data, resulting in time constants at $\Delta t_{25}$ = 1.9 ms, and at $\Delta t_{50}$ = 1.8 ms. (*B*) Time-course of recovery from delay at −80 mV. The time constant for $\Delta t_{50}$ is 2.1 ms, for $\Delta t_{25}$ is 1.5 ms. (*C*) Simulation of steady state delay vs. conditioning for a test pulse to +20 mV.

larger than for onset. This problem has not been investigated in detail, but it is likely that at least one more state must be added to the scheme shown in Reaction 2 to fit the frog node data.

In their original examination of the potassium current dynamics in squid axons, Cole and Moore (1960) showed that all conductance increases from rest could be fit best by $g_k = g_k n^6$, where the single variable of state $n$ was given by the HH form $dn/dt = \alpha(n - 1) - \beta n$. This expression can be cast into a linear kinetic reaction with seven configurations as follows:

$$1 \rightleftharpoons 2 \rightleftharpoons 3 \rightleftharpoons 4 \rightleftharpoons 5 \rightleftharpoons 6 \rightleftharpoons G. \qquad \text{(Reaction 3)}$$

To fit the data for strong hyperpolarizing conditioning, they kept the same form and increased the exponent of $n$ to 25. Again, this can be cast into a longer linear kinetic reaction scheme with 26 configurations.

Thus, the squid axon currents after hyperpolarization also require additional states in a linear kinetic model. Their superposition arises from the unique and constrained relationships for the rate constants, e.g., Moore and Cox (1976).

Although it is possible to fit the crayfish data with another model,[1] the fact that the linear kinetic reaction scheme subsumes all of our data by different but conveniently understood constraints on rate constants, makes the latter preferable to us. We think this also shows that the presence or absence of superposition does not dictate particular models.

We appreciate the aid of Drs. R. Joyner, M. Johnston, and S. Jaslove in computer programming and analysis, of E. Harris in instrumentation, and of D. Crutchfield for secretarial assistance. We are grateful to Drs. T. Begenisich, K. S. Cole, R. FitzHugh, R. French, L. Goldman, T. Hill, and E. Jakobsson for reading and making suggestions for improving the manuscripts.

This work was supported by a grant (NS 03437) from the National Institutes of Health.

*Received for publication 7 April 1981 and in revised form 14 August 1981.*

---

[1]Subunit sequence raised to a power. Another scheme to try is expansion of the HH open-closed variable into a triplex state. The scheme would be of form:

$$\left(C_1 \underset{\beta z}{\overset{\alpha z}{\rightleftharpoons}} C_2 \underset{\beta}{\overset{\alpha}{\rightleftharpoons}} 0\right) \qquad \text{(Reaction 4)}$$

where the subunit is in one of three states open (O) or closed ($C_1$ and $C_2$). When $x$ subunits are in state O, the channel is open. At rest and for depolarizations, $\alpha z \gg \beta z$, so that $C_1$ is depleted and the model simplifies to

$$\left(C_2 \underset{\beta}{\overset{\alpha}{\rightleftharpoons}} 0\right)^x \qquad \text{(Reaction 5)}$$

which is equivalent to the HH expression and superposition will follow. At hyperpolarized voltages, the $C_1$ state is preferred, causing delay in the onset of the opening after a jump to a test-depolarized voltage. With proper choice of rate constants, this model will also provide the general features of superposition with depolarization, and increased delay and nonsuperposition properties for hyperpolarized conditioning pulses. It has not been investigated as extensively as the previousl model.

## REFERENCES


Begenisich, T. 1979. Conditioning hyperpolarization delays in the potassium channels of myelinated nerve. *Biophys. J.* 27:257–266.

Cole, K. S., and J. W. Moore. 1960 *a*. Potassium ion current in the squid giant axon: dynamic characteristic. *Biophys. J.* 1:1–14.

Cole, K. S., and J. W. Moore. 1960 *b*. Ionic current measurements in the squid giant axon membrane. *J. Gen. Physiol.* 44:123–167.

Goldman, L., and C. L. Schauf. 1973. Quantitative description of sodium and potassium currents and computed action potentials in *Myxicola* giant axons. *J. Gen. Physiol.* 61:361–384.

Hill, T., and Y.-D. Chen. 1971 *a*. On the theory of ion transport across nerve membrane. II. Potassium ion kinetics and cooperability (with x = 4). *Proc. Natl. Acad. Sci. U.S.A.* 68:1711–1715.

Hill, T., and Y.-D. Chen. 1971 *b*. On the theory of ion transport across nerve membrane. III. Potassium ion kinetics and cooperativity (with x = 4, 6, 9). *Proc. Natl. Acad. Sci. U. S. A.* 68:2488–2492.

Hodgkin, A. L., and B. Katz. 1949. The effect of sodium ions on the electrical activity of the squid. *J. Physiol. (Lond.).* 108:37–77.

Hodgkin, A. L., and A. F. Huxley. 1952. A quantitative description of membrane current and its application to conduction and excitation in nerve. *J. Physiol. (Lond.)* 117:500–544.

Moore, J. W., and E. B. Cox. 1976. A kinetic model for the sodium conductance system in squid axon. *Biophys. J.* 16:171–192.

Moore, J. W., and S. H. Young. 1981. Dynamics of potassium ion currents in axon membranes: a reexamination. *Biophys. J.* 36:715–721.

Moore, J. W., and T. Narahashi. 1967. Tetrodotoxin's highly selective blockage of an ionic channel. *Fed. Proc.* 26:1655–1663.

Palti, Y., G. Ganot, and R. Stämpfli. 1976. Effect of conditioning potential on potassium current kinetics in the frog node. *Biophys. J.* 16:261–273.

Schauf, C. L., T. L. Pencek, and F. A. Davis. 1976. Potassium current kinetics in *Myxicola* axons. *J. Gen. Physiol.* 68:397–403.

Shrager, P. 1974. Ionic conductance changes in voltage clamped crayfish axons at low pH. *J. Gen. Physiol.* 64:666–690.

Van Harreveld, A. 1936. Physiological saline for crayfish. *Proc. Soc. Exp. Biol. Med.* 34:428–432.

Young, S. H. 1980. Potassium current dynamics in crayfish giant axons. Ph.D. thesis, Duke University, Durham, N.C.